Colossal magnetoresistance of $Nd_{2/3}Sr_{1/3}MnO_3$ ultrathin films grown on charge-ordered $Nd_{1/2}Ca_{1/2}MnO_3$ manganite

J. Laverdière, S. Jandl, and P. Fournier

Regroupement Québécois sur les Matériaux de Pointe, Département de Physique, Université de Sherbrooke, Sherbrooke, Canada J1K 2R1

(Received 11 November 2010; revised manuscript received 13 June 2011; published 19 September 2011)

We present a study of the interfacial interaction between a ferromagnetic metallic manganite in proximity to a charge-ordered manganite in a bilayer structure. Different thicknesses (2–45 nm) of ferromagnetic metallic $Nd_{2/3}Sr_{1/3}MnO_3$ (NSMO-1/3) were grown by pulsed laser ablation on charge-ordered $Nd_{1/2}Ca_{1/2}MnO_3$ (NCMO-1/2) with a fixed thickness of 175 nm on $SrTiO_3$ (001) substrates. Electrical transport and magnetization measurements in large magnetic fields show that the metal-insulator transition temperature decreases with the NSMO-1/3 thickness down to a critical value of 4–5 nm below which NSMO-1/3 remains insulating at low temperature. The critical thickness corresponds also to the largest magnetoresistance response with the conducting phase recovered easily under the application of a magnetic field as low as 1.5 T. The insulating phase observed for the ultrathin NSMO-1/3 film is attributed to the compressive strain and the magnetic interaction in the vicinity of the charge-ordered NCMO-1/2. Magnetic measurements also show that a significant portion of the NCMO-1/2 layer magnetizes at lower field. This is a clear example of a forced phase percolation by proximity effect.

DOI: 10.1103/PhysRevB.84.104434 PACS number(s): 75.70.Cn, 75.47.Gk, 75.25.Dk

I. INTRODUCTION

Since the discovery of colossal negative magnetoresistance,[1] manganese oxides of general formula $A_{1-x}B_xMnO_3$ have attracted great attention in the 1990s for their potential of application but also for challenging fundamental questions. Colossal magnetoresistance (CMR) is often characterized by a drop in resistivity of several orders of magnitude in the presence of a magnetic field and is observed in a large range of doping x.

From $x = 0.2$ to 0.45, many compounds exhibit a ferromagnetic metallic (FMM) phase below their Curie temperature T_C while presenting a semiconductorlike behavior in their paramagnetic phase at high temperatures.[2,3] The application of a magnetic field shifts T_C to higher temperatures and generates a high ratio of magnetoresistance (MR) near this metal-insulator transition. However, the magnetic field required to observe this MR remains too large for practical purposes.

At integer fraction values of doping, manganites can exhibit charge ordering (CO), $x = 1/2$ being the most stable of all.[4] The charge-ordered phase is insulating and is accompanied by a sharp enhancement of resistivity at the transition temperature T_{CO}. Concomitant structural, magnetic, and orbital phase transitions also occur at close temperatures. At T_{CO}, the unit cell is changing from an orthorhombic ($Pnma$) to a monoclinic ($P2_{1/m}$) symmetry and at Néel temperature, T_N, the so-called CE-type anti-ferromagnetic phase takes place.[5–7] This phase is ascribed as zig-zag ferromagnetic chains in ab plan aligned anti-ferromagnetically in all directions. By applying a magnetic field beyond H_C, one can melt the CO and recover a metallic and ferromagnetic phase. For example, in single crystals of $Nd_{0.5}Ca_{0.5}MnO_3$, H_C reaches 20 T.[6,7] In thin films[8] of the same material, this field can be suppressed substantially down to 7 T (Refs. 9–11) because of the substrate strains. Despite their huge change in resistance of several orders of magnitude for $H \sim H_C$, the large melting field of CO materials hinders once again the potential for applications.

Recent studies of ultrathin films gave some successful enhancement of the low-field magnetoresistance. By growing $La_{2/3}Sr_{1/3}MnO_3$ on different substrates, Mukhopadhyay *et al.*[12] have shown that the metallic $La_{2/3}Sr_{1/3}MnO_3$ converts into an insulator for 20-nm-thick films on $LaAlO_3$ (LAO) and 10-nm-thick films grown on $SrTiO_3$ (STO). As proposed by these authors, the LAO substrate is more efficient than STO in inducing the insulator phase owing to the compressive strain that bends the Mn-O-Mn bonds and thus suppresses double exchange. For both types of films, the MR ratios were higher than the bulk value with a maximum CMR ratio of $\mathrm{CMR} \equiv 100 \times |\rho(B) - \rho(0)|/\rho(B) \sim 4 \times 10^5\%$ for the 20-nm-thick film on LAO under 7 T. The insulating state, however, becomes too robust for lower thicknesses and the corresponding MR ratios decrease due to the existence of a dead magnetic layer in the vicinity of the substrate.[13]

In this paper, we present a different route to enhance the magnetoresistance of manganite materials at low field. We use the proximity of an ultrathin ferromagnetic metallic $Nd_{2/3}Sr_{1/3}MnO_3$ layer (NSMO-1/3) to a 175-nm buffer of charge-ordered $Nd_{1/2}Ca_{1/2}MnO_3$ (NCMO-1/2) to generate and tune large magnetoresistance at magnetic fields of the order of 1–2 T. We find that the top NSMO-1/3 layer goes through a metal-insulator transition for a critical thickness of 4–5 nm while remaining ferromagnetic. Moreover, magnetic data suggests that the NSMO-1/3 top layer affects the first nanometers of the NCMO-1/2 sublayer by lowering the field required to magnetize the NCMO-1/2. CMR ratios as large as $10^8\%$ are achieved at a critical thickness under an applied magnetic field of only 2 T.

II. SAMPLES AND EXPERIMENTS

The bilayer films of $Nd_{0.67}Sr_{0.33}MnO_3$ (NSMO-1/3) and $Nd_{0.5}Ca_{0.5}MnO_3$ (NCMO-1/2) were grown by pulsed laser ablation deposition on $SrTiO_3$ (001) at a temperature of 750 °C under 400 mTorr of molecular oxygen. At 8 cm from the substrate, stoichiometric targets were ablated by a KrF laser ($\lambda = 248$ nm) at a repetition rate of 7 Hz and a fluence of 1.3 J/cm^2 over a spot size of 0.1 cm^2. The resulting growth rate

is ∼0.7 Å/pulse for both materials, which has been evaluated from the thickness measurement of reference samples. The growth was followed by an *in situ* fast cooling (35 °C/min) from 750 to 500 °C under 400 Torr of O_2, followed by a 5 °C/min cooling ramp from 500 to 400 °C. All bilayers have been grown with the bottom insulating NCMO-1/2 at a fixed thickness of 175 nm while the thickness of the top layer of NSMO-1/3 has been varied from 2 to 45 nm. In addition, 175-nm-thick NCMO-1/2 and NSMO-1/3 monolayers have been grown under the same conditions for comparison. We have also investigated the impact of growth conditions. Comments on those results will be found at the end of the next section.

The resulting bilayers were checked by x-ray diffraction (Cu $K\alpha$) in the θ-2θ mode to evaluate their actual out-of-plane lattice parameters. Their magnetic properties were studied using a superconducting quantum interference device (SQUID) magnetometer MPMS-XL7 from Quantum Design with the magnetic field applied in the film plane. Resistivity as a function of magnetic field and temperature was measured using a physical properties measurement system (PPMS) from Quantum Design using a conventional four-probe technique, with a current of 50 nA. For very resistive samples, a two-point technique has been used together with 100-MΩ resistance in parallel and a high internal resistance current source. Sample resistance R is then related to the measured voltage by $R = [I/V - 1 \times 10^{-8}]^{-1}$. These two methods can be superimposed in our results without correcting factors, confirming that the contact resistance remains negligible compared to the high resistance of the sample. As a nondestructive probe for the quality of the charge-ordered NCMO layer and the possible impact of the top NSMO layer, Raman scattering has been performed in a backscattering configuration using a Labram-800 microscope spectrometer equipped with a nitrogen-cooled CCD detector giving 0.5 cm^{-1} resolution. We used a 632.8-nm (1.96 eV) He-Ne laser line with a 50× objective focusing on a 3-μm spot.

III. EXPERIMENTAL RESULTS

Typical room-temperature x-ray diffraction (XRD) spectra in the θ-2θ mode are shown in Fig. 1(a) for the region between 45° and 50°. Besides the STO substrate [200] peak, for all bilayers, one can only observe the presence of a NCMO-1/2 peak indexed as [040] and leading to an estimated b-axis length of 7.54 Å, in agreement with previous reports,[10,11,14] although the b axis seems slightly shorter in our sample than in Ref. 10 for a similar thickness (175 nm). Since the b-axis value in bulk NCMO-1/2 is $b = 7.5949$ Å (in the *Pnma* symmetry, one has also $a = 5.4037$ Å and $c = 5.3814$ Å)[6] at room temperature, our data confirms that NCMO-1/2 films are subjected to in-plane tensile strains when growing on STO substrates.

With a bulk b axis of 7.698 Å ($a = 5.4656$ Å and $c = 5.4501$ Å in the *Pnma* symmetry),[15] the NSMO-1/3 layer should be *compressively* strained by NCMO-1/2. The growth direction has also been supposed to be along (010). As expected, the NSMO [040] peak overlaps closely with the STO [200], preventing its observation in most of our spectra. Using the 45-nm NSMO-1/3 thin film, by slightly tilting the sample intentionally, we could detect the wide NSMO peak centered at 46.76° [see Fig. 1(b)].[16] We evaluate that our

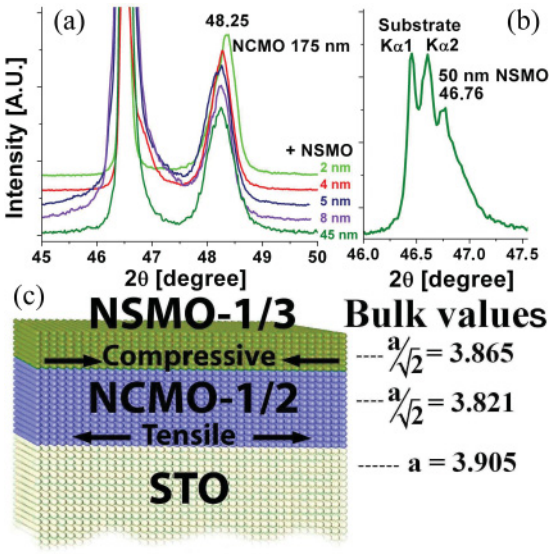

FIG. 1. (Color online) (a) X-ray diffraction patterns of several bilayers in the 45°–50° range. Values indicate the top $Nd_{2/3}Sr_{1/3}MnO_3$ (NSMO-1/3) film thickness. Only the x-ray diffraction peaks from the $Nd_{1/2}Ca_{1/2}MnO_3$ (NCMO-1/2) bottom layer are observable. (b) X-ray diffraction peaks after a slight tilt of a 45-nm NSMO-1/3 bilayer close to the [020] substrate peak. The first two peaks are from the substrate ($K\alpha_1$ and $K\alpha_2$) while the third one is from NSMO-1/3. (c) The outline of the expected strain effects in the bilayers.

ultrathin NSMO-1/3 layers have an expanded out-of-plane lattice parameter of at least 7.77 Å, hence showing strong compressive strain from the NCMO-1/2 bottom layer as expected. Strains are sketched in Fig. 1(c).

We performed atomic force microscopy (AFM) measurements on the surface of the NCMO-1/2 monolayer to characterize the surface roughness. This measurement is shown in Fig. 2. The surface is formed with islands of width varying from 50 to 120 nm. We find that the rms surface roughness is ∼1.8 nm and the average amplitude between peaks and valleys is ∼6 nm. In Figs. 2(b) and 2(c), one can see the surface profile along the white trace and black trace of Fig. 2(a) respectively. In Fig. 2(c) the profile is drawn with the same x and y scale. The gray line standing at 2 nm over the black line both in Figs. 2(b) and 2(c) has been added to give a visual perspective of the thickness of the NSMO-1/3 film compared with the surface roughness. For the thinnest NSMO-1/3 films of 2 nm, the roughness of the NCMO-1/2 buffer is important but likely insufficient to generate nonuniform (islandlike) growth.

Figure 3(a) shows resistance measurements from 5 to 300 K for different bilayers and a 200-nm monolayer of NSMO-1/3. The data for the NCMO-1/2 sample is not shown since it overlaps perfectly the trace of the 2-nm bilayer. Thicknesses indicated on the figure are the values for the NSMO-1/3 top layer, as we recall that the NCMO-1/2 bottom layer is kept at a constant thickness of 175 nm. The metal-insulator (*M-I*) transition, defined as the maximum of resistance, appears at a decreasing temperature as the NSMO-1/3 thickness is gradually reduced. In fact, this transition temperature is suppressed between NSMO-1/3 thicknesses of 4 and 5 nm (see below). The metalliclike regime is still apparent in the 5-nm film, even though resistance has built up significantly.

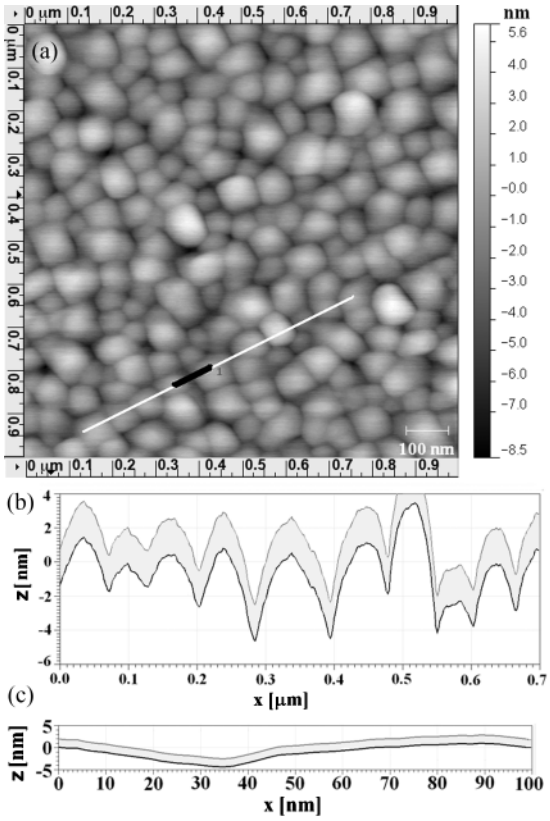

FIG. 2. (a) AFM scanning of the NCMO-1/2 monolayer sample on a 1 μm × 1 μm area. (b) Depth profile for the long (white) trace and (c) for the short (black) trace with the same x and z scaling. The gray line drawn above the black one in (b) and (c) illustrates the presence of a 2-nm film uniformly deposited on the surface.

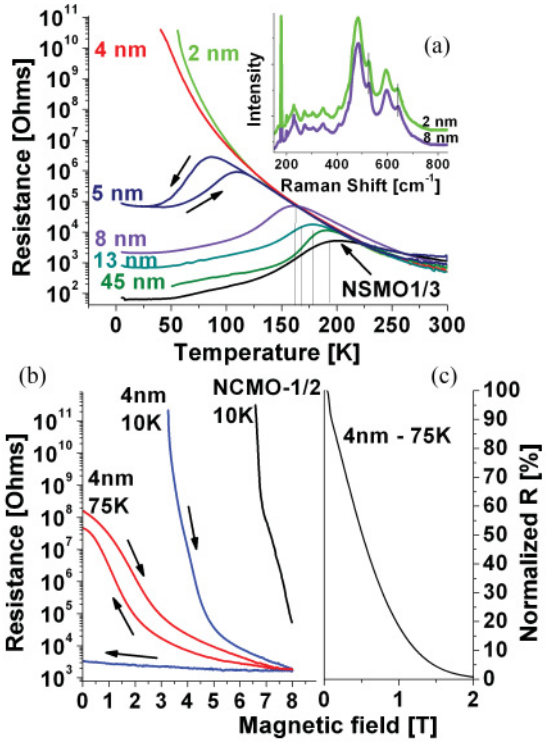

FIG. 3. (Color online) (a) Resistance as a function of temperature for the bilayers and a 200-nm monolayer of NSMO-1/3. Values give the thickness of NSMO-1/3. Inset: Raman scattering on bilayers made with 2 and 8 nm of NSMO-1/3 at 10 K. (b) Resistance as a function of magnetic field for selected temperatures for NCMO-1/2 and for a bilayer with 4 nm of NSMO-1/3. (c) Resistance ratio as a function of magnetic field in the region between 0 and 2 T for the bilayer with 4 nm of NSMO-1/3.

Moreover, we observe a temperature hysteresis at the onset of the *M-I* transition upon cooling ($T_{MI} = 86$ K) and warming ($T_{MI} = 109$ K). This hysteresis is only observed for that thickness and is vanishing for the 8-nm sample. The inset of Fig. 3(a) shows Raman scattering data obtained at 10 K on the 2- and 8-nm bilayers. The clear structures observed in these spectra are definite signatures of the charge and orbital ordered phase of NCMO-1/2 (Refs. 14,17, and 18) and are revealing the ordered phase persistence despite the presence of the NSMO-1/3 top layer. Since the light penetration depth in the NSMO-1/3 is ∼150 nm with the 50× objective, it is not possible to tell how Raman scattering in NSMO-1/3 is affected by its proximity with NCMO-1/2. The Raman signal from the CO layer is so strong that it prevents any possible distinction from the NSMO-1/3 signal. However, if non-negligible migration of Sr ions would occur, it would weaken and shift in frequency the CO-related modes as the one at 650 cm^{-1}. Since these modes are not affected when compared to a single layer of NCMO-1/2, we can rule out Sr/Ca migration.

The resistance as a function of magnetic field for the 4-nm bilayer for selected temperatures is presented in Fig. 3(b) and compared to a 175-nm CO film. At 10 K, a measurable resistance can be recovered for a magnetic field of roughly 3.5 T for the 4-nm bilayer. In contrast, the NCMO-1/2 monolayer resistance becomes measurable only from 7 T, clearly indicating that CO is weakened in the bilayer with respect to the monolayer. At 75 K (cooled from 300 K), the sample with 4 nm of NSMO-1/3 loses close to 50% of its resistance for only 0.5 T [as shown in Fig. 3(c)]. This very large low-field magnetoresistance is comparable to some CO/FM multilayers found in the literature[19,20] and to mixed compounds, characterized by strongly competing phases.[21]

Figures 4(a) and 4(b) show resistance measurements as a function of temperature under different magnetic fields for the two insulating bilayers, i.e., 2- and 4-nm-thick NSMO-1/3. The first striking feature is the very low field needed to recover the *M-I* transition [maximum in the $R(T)$ traces] for both samples. While it requires between 2 and 3 T to observe a maximum in the $R(T)$ traces in the case of the 2-nm bilayer, only 1.5 T is required for the 4-nm bilayer. Temperature hysteresis is also observable at the metal-insulator transition for the smallest thicknesses. This behavior is characteristic of the first-order phase transition, illustrating the competition between the ferromagnetic metallic and the charge-ordered phases.[22,23] Figure 4(c) shows a CMR ratio at 5 K $\leqslant T \leqslant$ 300 K under 2 T for several samples. We observe that the largest CMR is obtained for the critical NSMO-1/3 thickness of the 4-nm bilayer at more than 10^8%. The CMR is remaining large at 5 nm but is rapidly decreasing with thickness. In

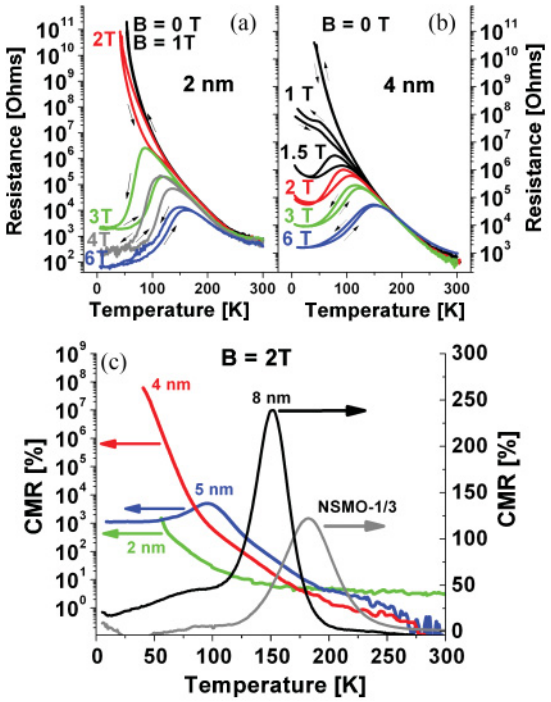

FIG. 4. (Color online) Resistance as a function of temperature in different magnetic fields for the bilayers with (a) 2 nm of NSMO-1/3 on top of NCMO-1/2 and (b) 4 nm of NMSO-1/3. (c) Colossal magnetoresistance ratio (see the text) as a function of temperature measured at a fixed magnetic field of 2 T.

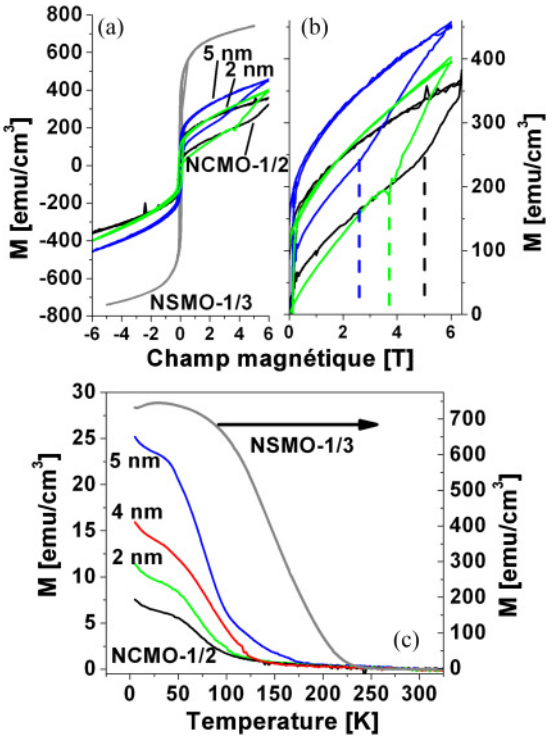

FIG. 5. (Color online) (a) Magnetization as a function of field at 5 K for an NSMO-1/3 monolayer, a NCMO-1/2 monolayer, and two bilayers with 2 and 5 nm of NSMO-1/3 on top of NCMO-1/2. (b) Magnified view showing the first magnetization branch for the same samples with the onset of additional magnetization at the dashed lines. (c) Magnetization as a function of temperature measured while cooling the samples under 500 Oe.

contrast, the NCMO monolayer did not show any significant CMR under 2 T at any temperature (not shown).

Magnetization loops at 5 K for two bilayers compared to NSMO-1/3 and NCMO-1/2 monolayers are shown in Figs. 5(a) and 5(b). For the charge-ordered NCMO-1/2 monolayer of 175-nm thickness, the first magnetization branch presents a weak ferromagneticlike magnetization at low fields up to the CO melting field (H_C) of roughly 5 T and is indicated by the dashed line. From that point, the magnetization raises until the field is reversed, suggesting one has not yet reached full saturation. At 6.5 T our NCMO-1/2 monolayer shows a magnetization value close to $2\mu_B$/Mn (350 emu/cm^3), way below the maximum saturation magnetization of $4.4\mu_B$/Mn (740 emu/cm^3) observed in the bulk.[7] The critical field seems lower in the magnetization measurements than in the resistance measurements [Fig. 4(b)], probably because the first FMM domains nucleate way before a first percolation path can be established throughout most of the NCMO-1/2 monolayer. After this first branch, the $M(H)$ curve resumes a fully reversible magnetization except at low fields ($H < 0.1$ T), with no sign of a transition back to the fully CO phase as is observed in single crystals.[7] This behavior has been often observed at low temperature in CO thin films[11,24] and indicates that areas of the films remain ferromagnetic and do not recover fully to the CO insulating phase, contrary to the bulk NCMO-1/2.[7] In Fig. 5(b), the effect of the NSMO-1/3 top layer on the magnetic response is to lower further the field H_C needed to magnetize the charge order (indicated by the dashed vertical lines).

Figure 5(c) shows the magnetization as a function of temperature in a small applied field (500 Oe) for the bilayers made with 2, 4, and 5 nm of NSMO-1/3. They are compared to the data obtained for the 200-nm-thick NSMO-1/3 and the 175-nm NCMO-1/2 monolayer. No hysteresis was observed for any sample. The magnetization of the bilayers is calculated using its total volume, including the NCMO-1/2 layer. The transition temperature corresponding to the onset of ferromagneticlike response increases quickly with the thickness of the top NSMO-1/3 layer. However, the additional ferromagnetic response observed for the 2-nm sample (~4 emu/cm^3) is sightly lower than the contribution expected for a fully polarized 2-nm-thick NSMO-1/3 (~8 emu/cm^3). This suggests that NCMO-1/2 hinders partly ferromagnetism in the insulating NSMO-1/3. In the case of the NCMO-1/2 film supposedly in the antiferromagnetic CO phase, the presence of a weak ferromagnetic response and no return to a full charge-ordered state at zero applied field may signal a magnetic contribution from the nonstoichiometry present at the interface between the substrate and the film as reported previously for $La_{2/3}Ca_{1/3}MnO_3$ grown on STO (001).[25]

In Fig. 6, we show the thickness dependence of the Curie temperature estimated from the $M(T)$ curves in Fig. 5(c), together with the *M-I* transition temperature defined as the maximum of the curves in Fig. 3(a). It suggests that the two characteristic temperatures track each other nicely except for

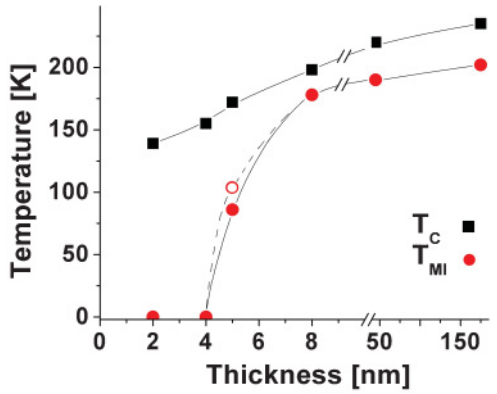

FIG. 6. (Color online) The metal-insulator transition temperature (T_{MI}) and the Curie temperature (T_C) as a function of the thickness of the top NSMO-1/3 layer. The open circle stands for T_{MI} measured by heating the sample.

small NSMO-1/3 thicknesses. The *M-I* transition collapses at a critical thickness of 4–5 nm while the layer preserves in part its ferromagnetic character.

Above the melting field H_C in single crystals,[7] the magnetization of NCMO-1/2 is expected to increase steeply and reach $\sim 4.4\mu_B$/Mn (740 emu/cm^3) as charge order is melted into a ferromagnetic metallic phase. In thin films, NCMO-1/2 can magnetize at a different field depending on the growth conditions. It has been reported by Rauwel Buzin *et al.*[11] how substrate temperature plays an important role on the stability of charge ordering. Our comparatively high-temperature deposition should rather stabilize charge order. But laser fluence also has an effect on the stoichiometry of the film.[26,27]

To further investigate how growth conditions may have an impact on the observed properties, especially the robustness of the CO phase, we changed the laser spot size on the target (thus the energy density). Additional NCMO-1/2 monolayers have been grown with 175-nm [Fig. 7(a)] and 250-nm [Fig. 7(b)] thicknesses using a smaller laser spot (energy density ~ 2.2 J/cm^2) and by measuring their magnetic properties before and between successive NSMO-1/3 layer deposition runs. For these growth conditions, charge ordering in NCMO-1/2 is more robust as the magnetization of the film is not observed for the 7-T field limit of our SQUID magnetometer [Figs. 7(a) and 7(b), lower trace], as was observed in Fig. 5(b). Only a weak hint of this transition can be perceived as the first magnetization branch does not overlap on top of the other branches. Moreover, as the field is decreased from 7 T, the sample retains a significant magnetization without recovering the initial CO state as in Fig. 5(b), hence indicating that ferromagnetic domains persist once again at low field, despite the improved robustness of CO. This irreversibility is in contrast to NSMO-1/3 monolayer [see Fig. 5(a)] in which first magnetization branch overlaps perfectly that of the following field sweeps above the saturation field ($\sim$700 Oe). The excess magnetization observed in NCMO-1/2 hence indicates that there is still a small portion of the NCMO-1/2 film that magnetizes under the 7-T field and persists at low fields.

For both NCMO-1/2 samples, we have deposited a 5-nm film of NSMO-1/3 followed by magnetization measurements.

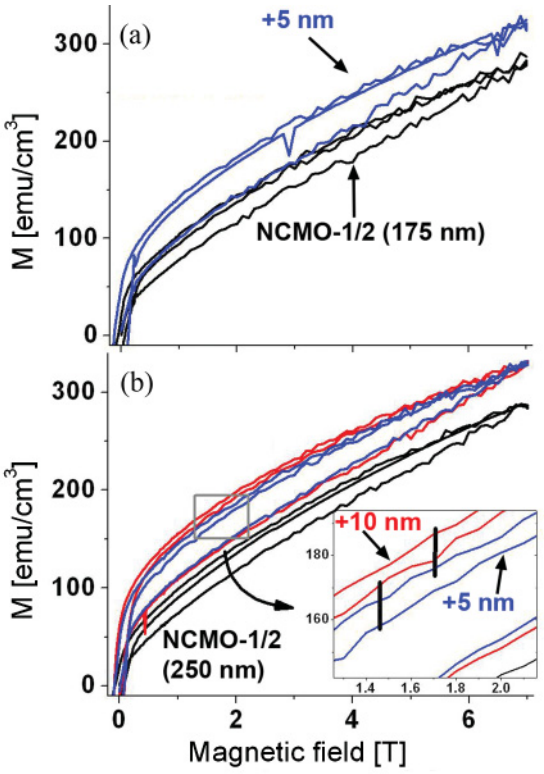

FIG. 7. (Color online) Magnetization as a function of applied magnetic field at 5 K for the successive steps of a bilayers of a 175-nm-thick (a) and a 250-nm-thick (b) NCMO-1/2 bottom layer (black traces) covered with a 5-nm (blue traces) and 10-nm (red trace) NSMO-1/3 layer. Inset: Magnified view of the region in the gray box. The vertical black lines are visual references with a 15 emu/cm^3 magnitude.

For the second sample, a subsequent 5-nm deposition of NSMO-1/3 has also been performed. When the first 5 nm of NSMO-1/3 is grown on the NCMO-1/2 [see Figs. 7(a) and 7(b)], the first magnetization branch is increased by 25 (35) emu/cm^3 for the 180- (255-) nm-thick sample. Additionally, the total magnetization at 7 T raises by roughly 35 (45) emu/cm^3. In both cases, 180- and 255-nm NCMO-1/2 layers, the contributions are more than what one would expect for 5 nm of fully polarized NSMO-1/3, i.e., $\sim$20 and 15 Oe/cm^3, respectively. This means that there is a larger portion of the NCMO-1/2 that magnetizes due to the proximity of the 5-nm-thick NSMO-1/3. A second 5-nm layer of NSMO-1/3 has been grown on the 250-nm-thick buffer of NCMO-1/2. This last deposition added only a weak excess of magnetization of roughly the expected magnitude (15 emu/cm^3). The vertical bars in the inset of Fig. 7(b) give a visual reference for 15 emu/cm^3, the contribution expected for a fully polarized 5-nm-thick NSMO-1/3 film. This last result with the second 5-nm layer compared to the magnetization with only the first layer is highlighting the impact of the first 5-nm film on the magnetic properties of the NCMO-1/2.

IV. DISCUSSION

The metal-insulator transition has already been reported in ferromagnetic metallic ultrathin films grown on insulating

substrates as $SrTiO_3$, $LaAlO_3$,[12,28,29] or $NdGaO_3$ (NGO).[13] The magnetoresistance ratio has been enhanced in these samples going from a few percents to thousands of percents. This enhancement was explained in terms of phase separation in $La_{2/3}Sr_{1/3}MnO_3$ (LSMO-1/3).[12] However, a dead magnetic layer, defined as the thinnest layer for which metallic and ferromagnetic behaviors are observed, prevents any useful magnetoresistance in very thin samples.[12,13,28] This dead magnetic layer in LSMO-1/3 is found to be 3 nm thick on LAO, 1.5 nm thick on NGO,[13] and 3 nm on STO,[28] although some discrepancies can be found in these thickness values.[12] In our configuration, the interface is quite different—that between NCMO-1/2 and NSMO-1/3.

The manifestation of the NSMO-1/3 insulating phase in our samples could be explained by two possible scenarios. A first scenario could involve the deposition of NSMO-1/3 itself. On a rough surface and for thin enough deposition, nonuniform deposition could lead to clusters (islands) of NSMO-1/3 isolated from each other in a matrix of NCMO-1/2, hence resulting in an insulating phase. For example, the NSMO-1/3 could deposit preferentially on hills or valleys in Fig. 2. However, a clear induction of a ferromagnetic phase within the NCMO-1/2 is observed in the magnetic measurements [Fig. 5(a)]. A good correspondence between NCMO-1/2 magnetization and the insulator-to-metal transition under magnetic field [Fig. 3(b)] combined with the decrease of T_C in the thin NSMO-1/3 bilayer suggests that the surface roughness scenario may be ruled out as the main origin of the transition.

The second scenario could be the direct interaction between NCMO-1/2 and NSMO-1/3. NCMO-1/2 compressive strain, as a LAO substrate, could induce an insulating phase with the NSMO-1/3. Some studies report that compressive strains would bend in-plane Mn-O-Mn bonds, resulting in orbital reconstruction and C-type antiferromagnetic ordering,[30,31] although this observation has been rejected by others.[28] From the double-exchange point of view, bending of the Mn-O-Mn bonds would favor antiferromagnetic superexchange to the detriment of double exchange, resulting in an insulating phase. However, the lattice mismatch between NCMO-1/2 and NSMO-1/3 is not very large (∼0.5%). Compressive strains alone may not be sufficient to explain the observation of an insulating phase. Magnetic interaction and local distortion of the NCMO-1/2 structure could also contribute to it. For instance, the CE-type antiferromagnetic ordering of NCMO-1/2 could inhibit double exchange in NSMO-1/3. In addition, Jahn-Teller distortion, supposed to be influent in the stabilization of charge ordering, could propagate into the NSMO-1/3 film and help to localize charges. Mechanical and magnetic interactions may link both materials. On the one hand, it gives an insulating phase in NSMO-1/3, and on the other hand, it induces ferromagnetic domains into the NCMO-1/2 as soon as a weak field is applied to magnetize the NSMO-1/3 thin film. The application of a magnetic field can then melt CO more easily at the interface.

Mixing of Sr and Ca ions could occur at the interface but remains very unlikely as an explanation of the insulating phase of NSMO-1/3. In $Pr_{0.65}Sr_{0.35}MnO_3$ (PSMO-0.35) single crystals,[32] Sr ions have to be replaced by over 50% of Ca ions before entering an insulating phase. Also, an increase in hole concentration in NSMO-1/3 would rather favor a ferromagnetic metallic phase. If intermixing of elements at the interface is the source of the insulating phase, it would indeed imply a very strong mixing through the interface. A mixing that large would also occur in NCMO-1/2, explaining the weakening of the NCMO-1/2 CO. But then this intermixing should have been observed in the Raman spectra by a shift and a decrease of intensity of the 650 cm^{-1} mode, a mode only observable in the long-range CO regime.[17,33] However, the Raman scattering of Fig. 2(a) shows that structures of NCMO-1/2 in either a 2- or 8-nm bilayer are not influenced by the presence of NSMO-1/3. It is worth noting that manganite multilayers are actively studied in literature.[19,34–40] Some heterostructures are grown at temperatures as high as 850 °C (Ref. 36) or 900 °C.[35] Our lower growth temperature, 750 °C, is commonly used as the growth temperature and intermixing is not reported as a significant issue. Moreover, our sample is bilayers. The second layer is also the last one to be grown. This means that the growth time of the thinnest NSMO-1/3 top layers leaves less time for ions to migrate across the interface. Hence we believe that interdiffusion cannot explain the results reported here.

Previous studies on multilayers presenting a pair of similar materials[19,20] have demonstrated good enhancement of MR around the *M-I* transition, but did not show any insulating phase. From their study of PCMO-1/3|LCMO-1/3 multilayers, Li *et al.*[20] suggest that MR enhancement had nothing to do with the CO. They rather explain their measurement with phase separation in the multilayer. In contrast, Venimadhav *et al.*[19] suggest that the enhancement of the magnetoresistance is due to a double-exchange mechanism induced in the charge-ordered material by applying a magnetic field. Here we clearly demonstrate that the charge-ordered material is modified by a ferromagnetic manganite neighbor, in agreement with the proposal of Venimadhav *et al.* Moreover, the phase separation scenario in manganites is still a matter of debate as to whether the phase separation is related to some composition inhomogeneities in the sample or that the electronic phases can intrinsically separate. We show in this paper that a phase (here the ferromagnetic phase) can actually percolate in the other phase (charge-ordered phase). Our results could be taken as a "forced" phase separation at the interface.

The possibility that NCMO-1/2 can be magnetized and can respond to such a low magnetic field explains why the insulating NSMO-1/3 is easier to destabilize as compared to ultrathin films directly grown on substrates. Our results suggest that NSMO-1/3 on NCMO-1/2 has also no dead layer, in contrast to the films grown directly on insulators such as LAO or STO. Controlling phase separation in manganites could be the key to use their fascinating physical properties. As we have shown, an appropriate control of the growth conditions can also help improving the CMR properties of the interface by tuning the melting field of the charge-ordered material. The use of a charge-ordered material as a buffer layer gives a strong response to a magnetic field and could be a valuable asset for potential magnetoresistant components.

V. CONCLUSION

We have grown ferromagnetic metallic $Nd_{2/3}Sr_{1/3}MnO_3$ on charge-ordered $Nd_{1/2}Ca_{1/2}MnO_3$ and find that for thicknesses

lower than 5 nm, $Nd_{2/3}Sr_{1/3}MnO_3$ becomes insulating. The metallic phase is recovered if the sample is subjected to a magnetic field as low as 1.5 T. We conclude that ferromagnetic domains of the $Nd_{2/3}Sr_{1/3}MnO_3$ seem to induce ferromagnetic order into the $Nd_{1/2}Ca_{1/2}MnO_3$ bottom layer at much lower field than it would be required for a $Nd_{1/2}Ca_{1/2}MnO_3$ monolayer.

ACKNOWLEDGMENTS

We thank M. P. Singh for many discussions, and S. Pelletier and M. Castonguay for their valuable technical support. This work is supported in part by the National Science and Engineering Research Council of Canada, Canadian Institute for Advanced Research, and the Fonds Québécois de la Recherche sur la Nature et les Technologies.

[1] R. Kusters, J. Singleton, D. Keen, R. McGreevy, and W. Hayes, Physica B **155**, 362 (1989).

[2] C. N. R. Rao, A. K. Cheetham, and R. Mahesh, Chem. Mater. **8**, 2421 (1996).

[3] M. Salamon and M. Jaime, Rev. Mod. Phys. **73**, 583 (2001).

[4] Y. Tokura and Y. Tomioka, J. Magn. Magn. Mater. **200**, 1 (1999).

[5] P. G. Radaelli, D. E. Cox, M. Marezio, and S.-W. Cheong, Phys. Rev. B **55**, 3015 (1997).

[6] F. Millange, S. de Brion, and G. Chouteau, Phys. Rev. B **62**, 5619 (2000).

[7] M. Tokunaga, N. Miura, Y. Tomioka, and Y. Tokura, Physica B **247**, 491 (1998).

[8] W. Prellier, P. Lecoeur, and B. Mercey, J. Phys. Condens. Matter **13**, R915 (2001).

[9] W. Prellier, C. Simon, A. M. Haghiri-Gosnet, B. Mercey, and B. Raveau, Phys. Rev. B **62**, R16337 (2000).

[10] E. Rauwel Buzin, W. Prellier, B. Mercey, C. Simon, and B. Raveau, J. Phys. Condens. Matter **14**, 3951 (2002).

[11] E. Rauwel Buzin, W. Prellier, B. Mercey, and S. Debrion, J. Cryst. Growth **275**, e2409 (2005).

[12] S. Mukhopadhyay, I. Das, and S. Banerjee, J. Phys. Condens. Matter **21**, 026017 (2009).

[13] J. Z. Sun, D. W. Abraham, R. A. Rao, and C. B. Eom, Appl. Phys. Lett. **74**, 3017 (1999).

[14] S. Charpentier, M. Gill-Comeau, S. Jandl, and P. Fournier, J. Phys. Condens. Matter **18**, 7193 (2006).

[15] Y. Guo, Y. Liu, K. Tao, H. Zhou, and R. Waplling, J. Solid State Chem. **148**, 236 (1999).

[16] This is possible because the substrate diffraction peak has a smaller full width at half maximum than the [040] peak of the NSMO-1/3 film. Its intensity can then be suppressed more strongly with a very slight tilt away from the Bragg condition than that of the film peaks.

[17] M. V. Abrashev, J. Bäckström, L. Börjesson, M. Pissas, N. Kolev, and M. N. Iliev, Phys. Rev. B **64**, 144429 (2001).

[18] S. Jandl, A. A. Mukhin, A. M. Balbashov, and V. Y. Ivanov, J. Phys. Condens. Matter **18**, 1667 (2006).

[19] A. Venimadhav, M. S. Hegde, V. Prasad, and S. V. Subramanyam, J. Phys. D **33**, 2921 (2000).

[20] H. Li, J. R. Sun, and H. K. Wong, Appl. Phys. Lett. **80**, 628 (2002).

[21] T. Wu and J. F. Mitchell, Appl. Phys. Lett. **86**, 252505 (2005).

[22] H. Kuwahara, Y. Tomioka, A. Asamitsu, Y. Moritomo, and Y. Tokura, Science **270**, 961 (1995).

[23] M. Uehara, S. Mori, C. H. Chen, and S.-W. Cheong, Nature (London) **399**, 560 (1999).

[24] E. Rauwel Buzin, W. Prellier, C. Simon, S. Mercone, B. Mercey, B. Raveau, J. Sebek, and J. Hejtmanek, Appl. Phys. Lett. **79**, 647 (2001).

[25] S. Estrade, J. M. Rebled, J. Arbiol, F. Peiro, I. C. Infante, G. Herranz, F. Sanchez, J. Fontcuberta, R. Cordoba, B. G. Mendis, and A. L. Bleloch, Appl. Phys. Lett. **95**, 072507 (2009).

[26] P. Orgiani, R. Ciancio, A. Galdi, S. Amoruso, and L. Maritato, Appl. Phys. Lett. **96**, 032501 (2010).

[27] T. Ohnishi, M. Lippmaa, T. Yamamoto, S. Meguro, and H. Koinuma, Appl. Phys. Lett. **87**, 241919 (2005).

[28] M. Huijben, L. W. Martin, Y.-H. Chu, M. B. Holcomb, P. Yu, G. Rijnders, D. H. A. Blank, and R. Ramesh, Phys. Rev. B **78**, 094413 (2008).

[29] A. Tebano, C. Aruta, P. G. Medaglia, F. Tozzi, G. Balestrino, A. Sidorenko, G. Allodi, R. De Renzi, G. Ghiringhelli, C. Dallera, L. Braicovich, and N. B. Brookes, Phys. Rev. B **74**, 245116 (2006).

[30] A. Tebano, C. Aruta, S. Sanna, P. G. Medaglia, G. Balestrino, A. A. Sidorenko, R. De Renzi, G. Ghiringhelli, L. Braicovich, V. Bisogni, and N. B. Brookes, Phys. Rev. Lett. **100**, 137401 (2008).

[31] G. Colizzi, A. Filippetti, F. Cossu, and V. Fiorentini, Phys. Rev. B **78**, 235122 (2008).

[32] Y. Tomioka and Y. Tokura, Phys. Rev. B **66**, 104416 (2002).

[33] M. Kim, H. Barath, S. L. Cooper, P. Abbamonte, E. Fradkin, M. Rübhausen, C. L. Zhang, and S.-W. Cheong, Phys. Rev. B **77**, 134411 (2008).

[34] J. Seo, W. Prellier, P. Padhan, P. Boullay, J.-Y. Kim, H. Lee, C. Batista, I. Martin, E. Chia, T. Wu, B.-G. Cho, and C. Panagopoulos, Phys. Rev. Lett. **105**, 167206 (2010).

[35] K. Gehrke, V. Moshnyaga, K. Samwer, O. Lebedev, J. Verbeeck, D. Kirilenko, and G. Van Tendeloo, Phys. Rev. B **82**, 113101 (2010).

[36] G. Campillo, M. E. Gomez, A. Berger, A. Hoffmann, R. Escudero, and P. Prieto, J. Appl. Phys. **99**, 08C106 (2006).

[37] O. Morán, M. E. Gomez, and J. G. Ramirez, J. Appl. Phys. **97**, 10K116 (2005).

[38] P. Padhan and W. Prellier, Phys. Rev. B **71**, 174419 (2005).

[39] P. Prieto, M. E. Gomez, G. Campillo, A. Berger, E. Baca, R. Escudero, F. Morales, J. Guimpel, and N. Haberkorn, Phys. Status Solidi A **201**, 2343 (2004).

[40] A. Venimadhav, M. Hedge, R. Rawat, I. Das, and M. E. Marssi, J. Alloys Compd. **326**, 270 (2001).